Proceedings of the XIII National School of Superconductivity, Lądek Zdrój 2007

Multifunctional $La_{0.7}Sr_{0.3}MnO_3$ $-YBa_2Cu_3O_7$ Heterostructures

P. Przyslupski[a], K. Dybko[a], A. Tsarou[a], K. Werner-Malento[a], M. Sawicki[a], F. Laviano[b], L. Gozzellino[b] and E. Mezzetti[b]

[a]Institute of Physics, Polish Academy of Sciences
al. Lotników 32/46, 02-668 Warszawa, Poland
[b]Dept. of Physics, Politecnico di Torino
corso Duca degli Abruzzi 24, 10129 Torino, Italy

Complex perovskite oxides exhibit a rich spectrum of functional responses such as: superconductivity, magnetism etc. Combination of different oxides in multilayered structures increases the number of physical responses. Heterogeneous oxide structures represent a new class of nanostructures. They consist of ferromagnetic $La_{0.67}Sr_{0.33}MnO_3$ (F-LSMO) manganite and superconducting $YBa_2Cu_3O_7$ (Sc-YBCO) cuprate. The interaction between the two order parameters gives rise to new physical effects. In this review we will discuss various physical effects obtained in the bilayer and trilayer heterostructures. For example, the LSMO/YBCO bilayer structures are used to study the mechanism of magnetic pinning. The other possibility is the fabrication of spin valve-like structures LSMO/YBCO/LSMO. The spin dependent transport in trilayer structure was studied taking into account crossed Andreev reflection and electron co-tunneling processes.

PACS numbers: 74.25.Ha, 74.78.Db, 74.72.Bk, 75.70.Cn

1. Introduction

The possibility of developing an electronic technology utilizing spin rather than charge degree of freedom shows recently a strong interest [1]. The spin valve is a configuration that can be used to control electrical transport through the spin degree of freedom of the charge carriers. Spin valves are multilayer devices composed of two ferromagnetics separated by nonmagnetic spacer (N) layer. Such device exhibits the effect of magnetoresistance (MR) that is the change in electrical resistance depending on the magnetic moment alignment of two ferromagnetic (F) electrodes. Replacing the nonmagnetic spacer layer by superconductor (S) the F/S/F superconducting spin valve is created [2]. The superconducting correlation in S layer could be controlled by the magnetization orientation in F layers. When normal metal is in contact with superconductor it acquires superconducting properties. This is known as the proximity effect (PE) and is explained in terms of the Andreev reflections [3]. Due to antagonism between ferromagnetism and superconductivity it is reasonable to expect that PE in F should be very short ranged. Surprisingly, some of the experiments [4] seem to be in contradiction with short-

-range nature of the PE in S/F structures. These models explain the long range PE by the formation of a strong triplet pairing amplitude component. Another possibility for long-range superconducting correlation penetration to a distance much longer than coherence length, $\xi_F \sim (hD/2E_{ex})^{1/2}$, is the effect of crossed Andreev reflection (CAR) [5–9] occurring in the vicinity of magnetic domain walls (DW). Recent report [10, 11] on LSMO/YBCO/LSMO trilayer structures demonstrate large magnetoresistance at temperatures in vicinity of superconducting transition temperature. In this work we investigate the MR effect in LSMO/YBCO/LSMO trilayer structures. In the case of YBCO/LSMO bilayer the main goal was to study the contribution of magnetic interaction to vortex nucleation and pinning in twinned YBCO/LSMO bilayers.

2. Experimental

$La_{0.7}Sr_{0.3}MnO_3/YBa_2Cu_3O_7$ and $La_{0.885}Sr_{0.115}MnO_3/YBa_2Cu_3O_7$ bilayer and LSMO/YBCO/LSMO trilayer structures were made using dc high pressure sputtering method [12, 13], onto (100) $LaAlO_3$ and (100) $[(LaAlO_3)_{0.3}(Sr_2TaAlO_6)_{0.7}]$ (LSAT) substrates. The $R(T)$ was measured using four-point method. $M(H)$ data were performed in SQUID magnetometer. The dynamical resistance characteristics were performed using low frequency lock-in. For the transport measurements the trilayer step-like structure was deposited.

Magneto-optical imaging with indicator film (MOIF) was performed by means of an optical microscope with polarization analysis and of an epitaxial Bi-doped iron garnet film [14]. The polarization plane of the light is locally rotated by the indicator in dependence on the local perpendicular magnetic field component due to the Faraday effect. Then the light contrast of the frame acquired by the camera, after the analyzer, is proportional to the magnetic field distribution induced by the sample [15, 16].

3. Results and discussion

3.1. Magneto-optical characterization of LSMO/YBCO bilayers

For the bilayer structure YBCO/LSMO/$LaAlO_3$ we studied the contribution of the magnetic interaction to vortex nucleation and pinning in twinned bilayers. MOIF measurements were performed on YBCO/LSMO bilayers grown on twinned $LaAlO_3$ substrates. The twin-boundaries (TB's) induce splitting of the manganite domain pattern, with out-of-plane domain walls that are pinned at the TB's and divide magnetic domains with in-plane magnetization [17]. It is worthy to note that the stray field generated by the magnetic microstructure of the manganite layer causes the nucleation of a spontaneous vortex and anti-vortex pattern in the superconducting layer when it is cooled below the T_c (in nominal zero field), as demonstrated by the measurement of a bilayer with $La_{0.67}Sr_{0.33}MnO_3$ layer presented in Fig. 1a. In presence of an external magnetic field (perpendicular to the film), the vortex diffusion in the bilayer is affected by the domain walls. Perpendicular TB's delay the vortex diffusion, but in de-

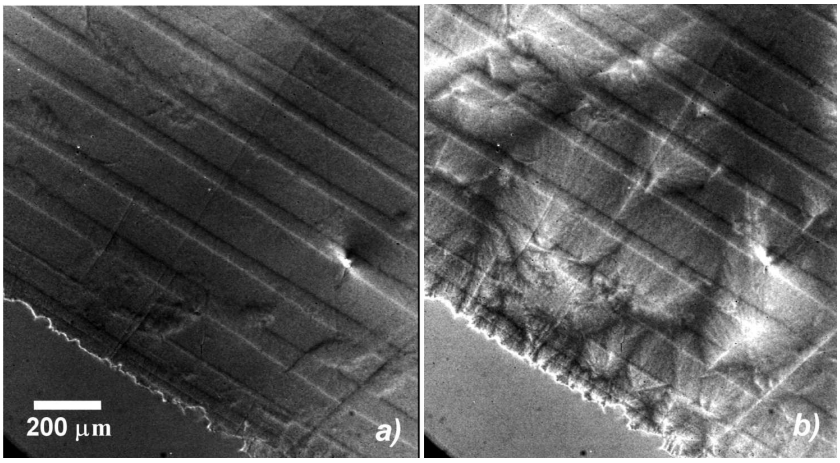

Fig. 1. B_z distributions measured at $T = 4.2$ K. (a) After zero external field cooling, domain walls are still visible since they spontaneously nucleate vortices in the superconducting layer. (b) Magnetic field pattern during vortex diffusion inside the YBCO induced by an external out-of-plane magnetic field $\mu_0 H_{\rm ext} = 3$ mT (directed upward).

pendence on the magnetization sign, the domain walls pile up or annihilate the moving vortices (Fig. 1b). Noticeably, in the case of vortices moving along the twins, the vortex diffusion results to be enhanced for the same sign of the domain--wall stray field and of the vortex field and become delayed for the opposite sign. This channeling phenomenon is observed in the middle of the sample area as presented in Fig. 2. This observation shows the possibility of the control of the vortex movement in the superconducting layer by means of the magnetization reversal in the underlying magnetic layer [17]. On the other hand, when the magnetization

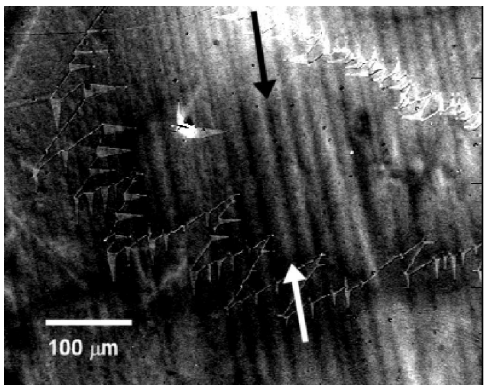

Fig. 2. Magnetic field distribution in the central part of the film ($T = 4.2$ K, $\mu_0 H_{\rm ext} = 4.5$ mT). Here vortices diffuse along the domain walls. The fork shape of the critical state pattern demonstrates that out-of-plane domain walls are blocking vortices of opposite polarity (black arrows) and are channeling those of the same sign (white arrows).

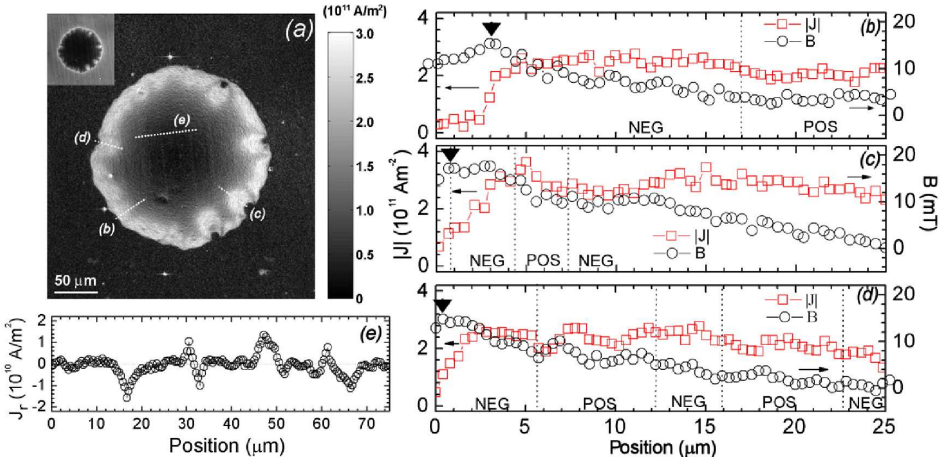

Fig. 3. (a) Supercurrent density modulus distribution at $T = 4.2$ K and $\mu_0 H_{\rm app} = 4.5$ mT, after zero field cooling (ZFC). In the inset the corresponding distribution of the magnetic field is presented. Parts (b)–(e) are supercurrent density and magnetic field line profiles traced along the corresponding dotted segments in the supercurrent density map in (a). Dotted vertical lines in (b), (c) and (d) mark the TB position and the downward triangle indicates the sample edge. The subscripts POS and NEG indicate that the out-of-plane magnetization component of the domains is directed parallel or antiparallel with respect to the applied field. The average current density over the POS domains is 2.403×10^{11} A m^{-2}, whereas over NEG domains it is 2.577×10^{11} A m^{-2}. For (e), data points are taken from the radial component (magnitude and sign) of the supercurrent distribution, along the corresponding dotted line traced in (a).

of the manganite domains is slightly tilted out-of-plane [18], we observed the interaction of vortices with bulk domains. The quantitative measurement of the electrical current density distribution for a disk shaped YBCO layer, deposited on the $La_{0.885}Sr_{0.115}MnO_3$ film is shown in Fig. 3a. The corresponding linear profiles are shown in Fig. 3b–d respectively. The critical current attains two different values (10% across the average critical current), in adjacent domains with opposite sign of the out-of-plane magnetization component. Moreover, this alternating magnetization is mirrored by alternating screening current loops measured in the sample center and shown in the current profile of Fig. 3e. The latter effect is due to the induction of spontaneous vortices and anti-vortices by alternating domains.

3.2. Transport and magnetic characterization of LSMO/YBCO/LSMO trilayers

First we have measured MR of the single LSMO film deposited on LSAT substrate. Magnetic field dependent MR of the LSMO thin film shows that MR peaks occur at the coercive field. The enhancement of low field MR of the manganite films is attributed to the spin dependent scattering [19, 20] or tunneling across grain

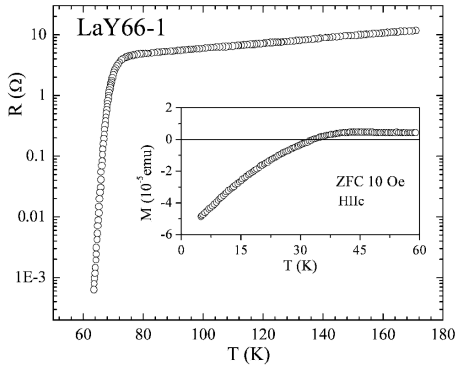

Fig. 4. Resistance vs. temperature of the LSMO(10 nm)/YBCO(19 unit cells)/ LSMO(24 nm) trilayer. Inset shows ZFC magnetic moment vs. temperature.

boundaries and /or magnetic domain walls. In Fig. 4 the resistance versus temperature is shown for the LSMO(10 nm)/YBCO(19 unit cells)/LSMO(24 nm) trilayer structure. The onset of the superconducting transitions begins at $T_{c0} = 72$ K. Inset in Fig. 4 shows the onset of the diamagnetic transition at $T_{d0} \approx 32$ K. The discrepancy between the T_{c0} and T_{d0} could be explained by the appearance in this temperature range of the spontaneous vortex lattice [21]. Magnetization hysteresis loops demonstrate that the saturation magnetic field is of about 650 Oe and the in-plane direction is the easy axis. The coercive magnetic field of the trilayer is of about 80 Oe. $M(H)$ measurements of the bottom LSMO layer shows that the saturation field of single LSMO(2.4 nm) layer is reached at about 350 Oe. The coercive field of the single layer is lower and equal to 20 Oe. Such feature demonstrates that applying the in-plane magnetic field first the magnetic moment of bottom LSMO layer became aligned with field. This means that above 350 Oe and below the saturation field of trilayer ($\approx$ 650 Oe) the upper LSMO layer (10 nm) is antiparallel aligned to the bottom layer. The upper layer became aligned parallel to the applied magnetic field at saturation field and also to the bottom LSMO layer. In Fig. 5 MR effect measured below the onset transition is presented. MR defined as $((R_{max} - R_{min})/R_{min}) \times 100\%$ for current-in-plane (CIP) geometry MR($T = 64.8$ K) $\approx 1000\%$ in CIP configuration. Our data demonstrate that the maximum of low field MR occurs at H_{co} field. At magnetic field below H_{co} the bottom and upper layers are composed of individual magnetic domains whose magnetization is in the plane and have some misalignment angles resulting in some net magnetic moment. As the magnetic field increases the average misalignment decreases first in the bottom LSMO layer. At the saturation field of the trilayer also in the upper LSMO layer the average domain misalignment decreases. In the measured sample the maximum of low field MR occurs at coercive field ($H \approx 80$ Oe), therefore it is reasonable to suppose that this effect is related to the spin dependent scattering at the grain boundaries and/or domain walls. As

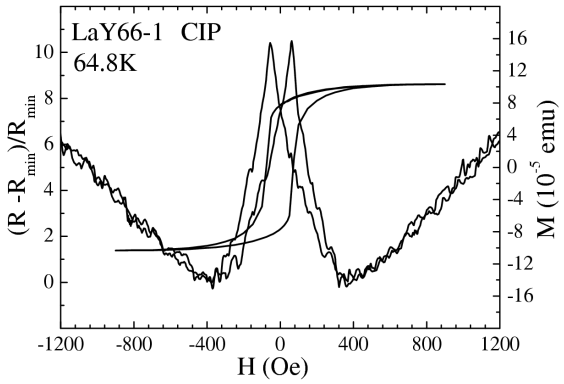

Fig. 5. MR vs. H of the trilayer measured with in-plane magnetic field. $M-H$ loop was measured at 64.8 K.

the magnetic field increases we observe minimum of the low field MR at about $H \approx 400$ Oe to 500 Oe. A possible source of spin dependent transport in the superconducting state is quasiparticle propagation below superconducting gap. It was predicted that in multiterminal structure the incident electron and the retroreflected hole might be transmitted through different contact as long as the distance between the contacts does not exceed the superconducting coherence length yielding a negative resistance. In another nonlocal process electron co-tunneling (EC) in which the electron enters the superconductor through one contact and electron of the same spin leaves through another contact yields a positive resistance. If the two contacts are spin polarized CAR and EC are favorable for antiparallel and parallel alignment of magnetic domains, respectively [7, 10, 11]. Referring such scenario to our samples it is possible that in our case the role of different contacts is played by magnetic domains, if the domain wall width is not larger than the $\xi_{ab} \approx 3$ nm. This value seems to be reasonable taking into account that the average size of the domains in LSMO film is of 14 nm to 28 nm [22]. $\mathrm{d}I/\mathrm{d}V$ vs. V data exhibit zero bias conductance peak (ZBCP) in favor of CAR process [23]. According to such scenario, for the LSMO/YBCO/LSMO trilayer, the low field MR peak occurs at the coercive field due to electron scattering at the domain wall or grain boundaries. As the magnetic field increases, the domain rearrangement results in parallel domain alignment in each LSMO layer. The observed minimum of MR presumably is a result of competition of two processes i.e. CAR and EC. For magnetic field below 500 Oe, dominating in the subgap transport is CAR effect resulting in negative MR. The increase in the magnetic field above 500 Oe results in switching of the magnetic moments of each LSMO layer to the parallel alignment, which is favorable for EC effect resulting in positive MR. We have measured the resistive transition in magnetic field as shown in Fig. 6. It is seen that the resistive transition in magnetic field of $H \approx 500$ Oe at $0.9R_{\mathrm{n}}$ (R_{n} resistance at the onset transition, T_{co}) lies of about 0.3 K above the transition in magnetic

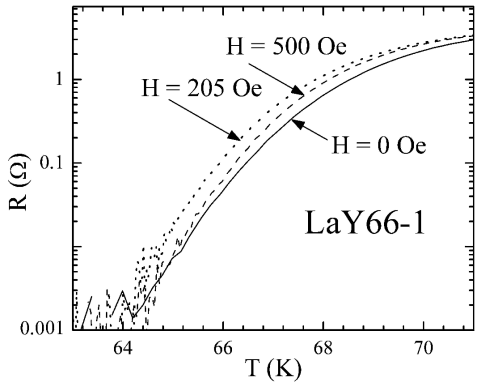

Fig. 6. The resistance vs. temperature measured with in-plane magnetic field $H = 0$, 500, and 205 Oe.

field of 205 Oe. This result shows that "degree of mutual antiparallel alignment of upper and bottom LSMO layers is higher at $H \approx 500$ Oe than at magnetic field of $H \approx 205$ Oe". Such effect was observed in metallic superconducting spin valve structure [24]. To summarize, we have investigated the low field magnetoresistance effect in LSMO/YBCO/LSMO trilayer structures. We have found that the low field MR peak occurs at coercivity field indicating the domain wall spin scattering process responsible for such feature. The source of minimum of MR results from the crossed Andreev reflection, which shunts [8] the LSMO layers. Above the saturation field the LSMO layers became aligned parallel, which favors the EC process yielding positive MR. This observation was also confirmed through superconducting spin switch effect, demonstrating higher transition temperature for magnetic field of about 500 Oe in comparison to the transition in lower magnetic field (of about 205 Oe) of the trilayer structure.

MOIF studies of twinned YBCO/LSMO demonstrate nonzero magnetic flux generated by the LSMO layers, which is frozen in YBCO layer when sample is cooled below the superconducting transition temperature. The intrinsic pinning of TB's on vortices is modulated by the localized magnetic moment of LSMO layer in such a way that vortices channeling along TB can be pushed ahead or backward in dependence on the orientation of the DW magnetization with respect to the external field that generates the new vortices. When bilayer displays out-of-plane magnetic domain and in-plane DW a modulation of the critical current ($\approx 10\%$) and new supercurrent pattern in the shielded region is observed.

Acknowledgments

This work was supported by the Ministry of Sciences and Higher Education under research project for the years 2006–2009 (MNiSW — 1 P03B 122 30) and by the Network "New materials and sensors for optoelectronics, information technology, energetics and medicine". This work was also partially supported by

the Programme of Scientific and Technological Cooperation between the Italian Republic and the Republic of Poland 2004–2006.

References

[1] S.A. Wolf, P.D. Awschalon, R.A. Burnn, *Science* **294**, 1488 (2001).

[2] L.R. Tagirov, *Phys. Rev. Lett.* **83**, 2058 (1999).

[3] A.F. Andreev, *Zh. Eksp. Teor. Fiz.* **46**, 1823 (2064).

[4] R.S. Keizer, S.T. Goennenwein, T.M. Klapwijk, G.Miao, G. Xiao, A. Gupta, *Nature* **439**, 825 (2006).

[5] G. Dutscher, D. Feinberg, *Appl. Phys. Lett.* **76**, 487 (2000).

[6] P.A. Aronow, G. Koren, *Phys. Rev. B* **72**, 184515 (2005).

[7] D. Beckmann, H.B. Weber, H. Lohneysen, *Phys. Rev. Lett.* **93**, 197003 (2004).

[8] F. Giazotto, F. Taddei, F. Beltram, *Phys. Rev. Lett.* **97**, 87001 (2006).

[9] N. Stefanakis, R.J. Melin, *J. Phys., Condens. Matter* **15**, 4239 (2003).

[10] V. Pena, Z. Sefrioui, D. Arias, C. Leon, J. Santamaria, J.L. Martinez, S.G.E. te Velthuis, A. Hoffman, *Phys. Rev. Lett.* **94**, 57002 (2005).

[11] C. Visani, V. Pena, J. Garcia-Baricanall, D. Arias, Z. Sefrioui, C. Leon, J. Santamaria, N.M. Nemes, M. Garcia Hernandez, J.L. Martinez, S.G.E. te Velthuis, A. Hoffman, *Phys. Rev. B* **75**, 54501 (2007).

[12] P. Przyslupski, I. Komissaarov, W. Paszkowicz, P. Dluzewski, R. Minikayev, M. Sawicki, *Phys. Rev. B* **69**, 34428 (2004).

[13] P. Przyslupski, *Phys. Status Solidi C* **5**, 1625 (2005).

[14] Ch. Jooss, J. Albrecht, H. Kuhn, S. Leonhardt, H. Kronmuller, *Rep. Prog. Phys.* **65**, 651 (2002).

[15] F. Laviano, D. Botta, A. Chiodoni, R. Gerbaldo, G. Ghigo, L. Gozzelino, S. Zannella, E. Mezzetti, *Supercond. Sci. Technol.* **16**, 71 (2003).

[16] F. Laviano, L. Gozzelino, R. Gerbaldo, G. Ghigo, E.Mezzetti, P. Przyslupski, A. Ttsarou, A. Wisniewski, *Phys. Rev. B* **76**, 214501 (2007).

[17] F. Laviano, L. Gozzelino, E. Mezzetti, P. Przyslupski, A. Tsarev, A. Wisniewski, *Appl. Phys. Lett.* **86**, 152501 (2005).

[18] L. Gozzelino, F. Laviano, P. Przyslupski, A. Tsarou, A. Wisniewski, D. Botta, R. Gerbaldo, G. Ghigo, *Supercond. Sci. Technol.* **19**, S50 (2006).

[19] J. Wolfmann, A.M. Haghiri-Gosnet, B. Raveau, C. Vieu, Combrill, A. Cornette, H. Launois, *J. Appl. Phys.* **89**, 6955 (2001).

[20] S.Y. Yang, W.L. Kuang, Y. Liou, W.S. Tse, S.F. Lee, Y.D. Yao, *J. Magn. Magn. Mater.* **268**, 326 (2004).

[21] P. Przyslupski, I. Komissaarov, W. Paszkowicz, P. Dluzewski, R. Minikayev, M. Sawicki, *J. Appl. Phys.* **95**, 2906 (2004).

[22] O.I. Lebedev, J. Verbeeck; G. Van-Tendeloo, S. Amelinckx, F.S. Razavi; H-U. Habermeier, *Philos. Mag. A* **81**, 797 (2001).

[23] K. Dybko, A. Tsarou, K. Werner-Malento, M. Sawicki, P. Przyslupski, in preparation.

[24] J.Y. Gu, C.Y. You, J.S. Jiang, J. Pearson, Ya.B. Bandly, S.D. Bader, *Phys. Rev. Lett.* **89**, 267001 (2002).